

AD743058

NAVAL RESEARCH AND DEVELOPMENT CENTER

Hampton, Virginia 23364

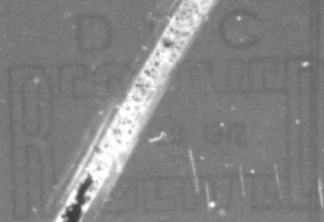


THE TOPSOIL AND TOPSOIL POLYMER LAYER
OF BENTONITE DEMONSTRATES HIGH STRENGTH AND STIFF SURFACE,
AND INCREASED PERMEABILITY SOLUTIONS

John S. Grandjean

APPROVED FOR PUBLIC RELEASE - DISTRIBUTION UNLIMITED

SHIP PERFORMANCE DEPARTMENT
RESEARCH AND DEVELOPMENT CENTER



Reproduced by
**NATIONAL TECHNICAL
INFORMATION SERVICE**
Springfield, Va. 22151

THE UNIVERSITY OF CHICAGO
DEPARTMENT OF CHEMISTRY
530 SOUTH EAST ASIAN AVENUE
CHICAGO, ILLINOIS 60607

ORGANIZATIONAL CHART

PROFESSOR
OF CHEMISTRY

ASSISTANT PROFESSORS

ASSISTANT PROFESSOR
OF CHEMISTRY

ASSISTANT PROFESSOR
OF CHEMISTRY

ASSISTANT PROFESSOR
OF CHEMISTRY

ASSISTANT PROFESSOR
OF CHEMISTRY

ASSISTANT PROFESSOR
OF CHEMISTRY

ASSISTANT PROFESSOR
OF CHEMISTRY

ASSISTANT PROFESSOR
OF CHEMISTRY

ASSISTANT PROFESSOR
OF CHEMISTRY

ASSISTANT PROFESSOR
OF CHEMISTRY

ASSISTANT PROFESSOR
OF CHEMISTRY

ASSISTANT PROFESSOR
OF CHEMISTRY

UNCLASSIFIED

Security Classification

DOCUMENT CONTROL DATA - R & D

(Security classification of title, body of abstract and indexing annotation must be entered when the overall report is classified)

1. ORIGINATING ACTIVITY (Corporate author) Naval Ship Research and Development Center Bethesda, Maryland 20034		2a. REPORT SECURITY CLASSIFICATION UNCLASSIFIED	
		2b. GROUP	
3. REPORT TITLE THE TORQUE AND TURBULENT BOUNDARY LAYER OF ROTATING DISKS WITH SMOOTH AND ROUGH SURFACES, AND IN DRAG-REDUCING POLYMER SOLUTIONS			
4. DESCRIPTIVE NOTES (Type of report and inclusive dates)			
5. AUTHOR(S) (First name, middle initial, last name) Paul S. Granville			
6. REPORT DATE April 1972		7a. TOTAL NO. OF PAGES 54	7b. NO. OF REFS 24
8a. CONTRACT OR GRANT NO.		9a. ORIGINATOR'S REPORT NUMBER(S) 3711	
b. PROJECT NO. R023-01		9b. OTHER REPORT NO(S) (Any other numbers that may be assigned this report)	
c.			
d.			
10. DISTRIBUTION STATEMENT Approved for public release: Distribution unlimited			
11. SUPPLEMENTARY NOTES		12. SPONSORING MILITARY ACTIVITY Naval Ship Systems Command	
13. ABSTRACT The resisting torque of disks rotating in an unbounded fluid is analyzed on the basis of three-dimensional boundary-layer theory. Smooth and rough surfaces in ordinary fluids and in drag-reducing polymer solutions are considered. A general logarithmic relation is derived for the torque as a function of Reynolds number for arbitrary roughness and arbitrary drag reduction. Special formulas are obtained for smooth surfaces, fully rough surfaces, polymer solutions with a linear logarithmic drag-reduction characterization, and polymer solutions with maximum drag reduction. Relations are also obtained for boundary-layer parameters such as thickness, wall shearing stress, etc. The computed results are in excellent agreement with experimental data available in the literature.			

UNCLASSIFIED

Security Classification

14. KEY WORDS	LINK A		LINK B		LINK C	
	ROLE	WT	ROLE	WT	ROLE	WT
Rotating disks; rough surfaces; drag reduction; polymer solutions						

DEPARTMENT OF THE NAVY
NAVAL SHIP RESEARCH AND DEVELOPMENT CENTER
BETHESDA, MD. 20034

THE TORQUE AND TURBULENT BOUNDARY LAYER
OF ROTATING DISKS WITH SMOOTH AND ROUGH SURFACES,
AND IN DRAG-REDUCING POLYMER SOLUTIONS

by

Paul S. Granville



APPROVED FOR PUBLIC RELEASE: DISTRIBUTION UNLIMITED

April 1972

Report 3711

TABLE OF CONTENTS

	Page
ABSTRACT	1
ADMINISTRATIVE INFORMATION	1
INTRODUCTION	1
GENERAL ANALYSIS	4
MOMENTUM EQUATIONS	4
RESISTING MOMENT OR TORQUE	6
CIRCUMFERENTIAL VELOCITY PROFILE	6
RADIAL VELOCITY PROFILE	8
SOLUTION OF MOMENTUM EQUATIONS	10
LOGARITHMIC MOMENT FORMULAS	14
GENERAL	14
SMOOTH SURFACES IN ORDINARY FLUIDS	16
ROUGH SURFACES OR DRAG-REDUCING POLYMER SOLUTIONS	17
SPECIAL LOGARITHMIC MOMENT FORMULAS	18
FULLY ROUGH SURFACES	18
ENGINEERING ROUGHNESS	19
POLYMER SOLUTIONS WITH LINEAR LOGARITHMIC CHARACTERIZATION	20
SURFACE WITH LAMINAR AND TURBULENT FLOW	21
LOCAL SKIN FRICTION	22
BOUNDARY-LAYER THICKNESS	23
ORDINARY BOUNDARY-LAYER THICKNESS	23
DISPLACEMENT THICKNESS	25
MOMENTUM THICKNESS	26
SHAPE PARAMETER	27
COMPARISONS WITH EXPERIMENTAL DATA	28
EVALUATION OF VELOCITY INTEGRALS	28
SOURCES OF EXPERIMENTAL DATA	29
VELOCITY PROFILES	30
SKEWNESS OF VELOCITY	31
LOCAL SKIN FRICTION	31
SKEWNESS OF WALL SHEAR STRESS	32
RESISTING MOMENT	32
RESISTING MOMENT FOR CASE OF MAXIMUM DRAG REDUCTION WITH POLYMER SOLUTION	33
APPENDIX - GENERAL POWER-LAW ANALYSIS FOR <i>SMOOTH</i> CASE	39
REFERENCES	42

LIST OF FIGURES

	Page
Figure 1 - Geometry of Flow and Coordinate System	35
Figure 2 - Radial Velocity Profile Comparison for Smooth Case, R = 4.2×10^6	36
Figure 3 - Radial Velocity Profile Comparison for Smooth Case, R = 2×10^6	36
Figure 4 - Comparison of Models of Relative Skewness of Flow	36
Figure 5 - Variation of Local Skin Friction Parameter σ with Reynolds Number for the Smooth Case	37
Figure 6 - Variation of Skewness of Wall Shear Stress with Reynolds Number for the Smooth Case	37
Figure 7 - Moment Coefficient versus Reynolds Number for the Smooth Case	38
Figure 8 - Maximum Drag Reduction with Polymer Additives	38

NOTATION

A	Slope of logarithmic velocity law in natural logarithms
\tilde{A}	A defined for interactive layer
A_1	Slope of logarithmic velocity law in common logarithms
\tilde{A}_1	$\tilde{A}_1 = 2.3026 \tilde{A}$
A	Factor in torque formula, Equation (71)
\tilde{A}	Factor in torque formula, Equation (160)
A_1	Factor in torque formula for fully rough surfaces, Equation (81)
a_0, a_1, a_2	Constants in series expansion, Equation (56)
\tilde{B}	Intercept of interactive logarithmic velocity law, Equation (159)
B_1, B_2	Intercepts of logarithmic velocity law, Equations (18) and (19)
B_3	Constant in Equation (75)
B'_1	Derivative of B_1 with respect to $\ln \ell^*$
B	Factor in torque formula, Equation (71)
\tilde{B}	Factor in torque formula, Equation (160)
B_1	Factor in torque formula for fully rough surfaces, Equation (79)
b_0, b_1, b_2	Constants in series expansion, Equation (55)
C_f	Coefficient of local skin friction
C_m	Torque coefficient, Equation (15)
c_1, c_2	Constants in Equation (70)
c_3, c_4	Constants in Equation (100)
c_5, c_6	Constants in Equation (101)
D	Constant, Equation (69)
F	Outer law function, Equation (17)
\tilde{F}	Integral of F with respect to z/δ , Equation (117)
\tilde{F}^2	Integral of F^2 with respect to z/δ , Equation (24)
$\tilde{F}g, \tilde{F}^2g, \tilde{F}g^2$	Integral of Fg, F^2g, Fg^2 with respect to z/δ respectively
\tilde{FG}	Integral of FG with respect to z/δ

g	Radial velocity law, Prandtl form, Equation (37)
$\frac{g^2}{g}$	Integral of g^2 with respect to z/δ
H	Shape parameter
h_1, h_2, h_3	Ratios given in Equations (40), (41), and (42)
k	Roughness linear dimension
k^*	Roughness Reynolds number, $k^* \equiv u_{\tau, \phi} k / \nu$
k_m	Torque coefficient, Equation (13)
l	Length measure
l^*	Length Reynolds number, $l^* \equiv u_{\tau, \phi} l / \nu$
l_o^*	Threshold value of l^* for polymer solutions
M	Moment or torque
m	Exponent in Equation (51)
P	Factor in Equation (84)
P_1, P_2	Factors in Equations (103) and (104)
P_{rr}	Normal stress in radial direction
$P_{\phi\phi}$	Normal stress in circumferential direction
P_{rz}	Shear stress in r-z plane
$P_{r\phi}$	Shear stress in r- ϕ plane
$P_{z\phi}$	Shear stress in z- ϕ plane
q	Drag reducing factor in Equation (69)
R	Reynolds number, $R \equiv \omega r^2 / \nu$
R_s	Reynolds number, $R \equiv \omega r^2 / \nu_s$
r	Radial distance from center of disk
s_1, s_2	Factors in Equation (111)
s_3, s_4	Factors in Equation (122)
s_5, s_6	Factors in Equation (131)
t	Subscript denoting transition
U	Relative velocity outside boundary layer, $U = \omega r$
u	Relative velocity inside boundary layer for circumferential direction

$u_{\tau,r}$	Shear velocity in radial direction, $u_{\tau,r} = \sqrt{\tau_{\omega,r}/\rho}$
$u_{\tau,\phi}$	Shear velocity in circumferential direction, $u_{\tau,\phi} = \sqrt{\tau_{\omega,\phi}/\rho}$
v_r	Velocity component in radial direction
v_ϕ	Velocity component in circumferential direction
v_z	Velocity component in normal direction
w	Coles wake function
z	Normal distance from disk
α	Tangent of angle of resultant wall shear stress from circumferential direction
α'	Derivative of α with respect to σ
β	Function given in Equation (47)
β'	Derivative of β with respect to σ
δ	Boundary layer thickness
δ^*	Displacement thickness
η	z/δ
θ	Momentum thickness
θ_1	Factor defined in Equation (130)
λ	Function given in Equation (54)
λ'	$d\lambda/d\sigma$
μ	Viscosity of fluid (solvent for polymer solution)
ν	Kinematic viscosity of fluid (solvent for polymer solution)
ν_s	Kinematic viscosity of solution for polymer solutions
ρ	Density of fluid
σ	Local skin friction parameter, $\sigma \equiv U/u_{\tau,\phi}$
$\tau_{w,r}$	Wall shear stress in radial direction
$\tau'_{w,\phi}$	Driving wall shear stress in circumferential direction
$\tau_{w,\phi}$	Wall shear stress in circumferential direction
ϕ	Azimuth angle
ψ	Skewness of velocity, Equation (148)
ω	Angular velocity

ABSTRACT

The resisting torque of disks rotating in an unbounded fluid is analyzed on the basis of three-dimensional boundary-layer theory. Smooth and rough surfaces in ordinary fluids and in drag-reducing polymer solutions are considered. A general logarithmic relation is derived for the torque as a function of Reynolds number for arbitrary roughness and arbitrary drag reduction. Special formulas are obtained for smooth surfaces, fully rough surfaces, polymer solutions with a linear logarithmic drag-reduction characterization, and polymer solutions with maximum drag reduction. Relations are also obtained for boundary-layer parameters such as thickness, wall shearing stress, etc. The computed results are in excellent agreement with experimental data available in the literature.

ADMINISTRATIVE INFORMATION

This investigation was conducted under the General Hydromechanics Research Program of the Naval Ship Systems Command. Funding was provided under Project R 023-01. Material in this report appeared informally as NSRDC Technical Note HL 133 in June 1969.

INTRODUCTION

A circular disk rotating in an unbounded fluid at rest develops a resisting torque, or moment, which is wholly viscous in origin. A boundary layer develops on the disk surface which is three-dimensional in that there is a cross-flow velocity component, namely, the radial velocity component. The boundary-layer flow is laminar at the center of the disk and undergoes transition to a turbulent flow at some radial distance from the center. The turbulent boundary layer on the disk behaves like other turbulent shear flows in another important aspect: there is increased resistance due to surface roughness and decreased resistance due to the presence of polymer additives in the fluid.

The principal aim of this report is to develop analytical relations between the resisting torque coefficient and the disk Reynolds numbers for the case of roughness and/or polymer additives in terms of boundary-layer factors. The relations between magnitude and direction of local skin friction (wall shearing stress) and Reynolds number also result. The basis

of the analysis is the similarity-law correlation for roughness and/or polymer additives. If the empirical factors in the similarity-law correlation are known, the torque and other properties of the flow may be predicted. Conversely, if the torque coefficient and Reynolds number are measured, the similarity-law empirical factors may be deduced. This is a most valuable attribute since the rotating disk may then be used as an instrument for experimentally obtaining similarity-law correlations for various types of irregular roughnesses and/or polymer additives at high shearing stresses. Once a similarity-law correlation is known, it may be used to predict the characteristics of other types of shear flows.^{1,2}

The development of resisting torque on the rotating disk depends on the development of the boundary layer on the disk, particularly the turbulent boundary layer at high Reynolds numbers. As originally formulated by von Kármán,³ the method of integral relations is based on the integration of the equations of motion across the boundary layer for both the circumferential and the radial directions. It is then necessary to supply relations for the circumferential and radial velocity components.

In the classical analyses of von Kármán³ and Goldstein⁴ for *smooth* surfaces, the circumferential velocity relative to the rotating disk is considered, in effect, to behave like an ordinary two-dimensional similarity-law shear flow except that the reference shear velocity is the skewed or resultant shear velocity. Von Kármán used a power-law similarity law and Goldstein the more general logarithmic similarity law. Von Kármán assumed

1. Granville, P.S., "The Frictional Resistance and Turbulent Boundary Layer of Rough Surfaces," *Journal of Ship Research*, Vol. 2, No. 3 (Dec 1958).

A complete list of references is given on pages 42 to 44.

2. Granville, P.S., "The Frictional Resistance and Velocity Similarity Laws of Drag-Reducing Polymer Solutions," *Journal of Ship Research*, Vol. 12, No. 3 (Sep 1968).

3. von Kármán, T., "On Laminar and Turbulent Friction," National Advisory Committee for Aeronautics TM 1092 (Sep 1946); translated from *Zeitschrift für angewandte Mathematik und Mechanik*, Vol. 1, No. 4 (Aug 1921).

4. Goldstein, S., "On the Resistance to the Rotation of a Disc Immersed in a Fluid," *Proceedings of Cambridge Philosophical Society*, Vol. 31, Pt. 2, p. 232 (Apr 1935).

that the radial velocity component was proportional to the *relative* circumferential velocity component and the skewness of the wall shearing stress, with a linear correction to provide zero velocity at the edge of the boundary layer. Goldstein, on the other hand, assumed that the radial velocity component (except very close to the wall) was proportional to the *absolute* circumferential velocity component, which automatically provides zero velocity at the edge of the boundary layer. Comparison with experimental data shows that the von Kármán model overestimates the radial velocity component whereas the Goldstein model grossly underestimates it. As stated before, the von Kármán and Goldstein analyses apply only to smooth surfaces. Dorfman^{5,6} extended the Goldstein analysis to the special case of the fully rough surface.

In the approach followed here, the boundary layer on the rotating disk is considered as a three-dimensional boundary layer. The streamwise velocity component in the boundary layer is then the circumferential velocity and the cross-flow velocity component is the radial velocity. The similarity law for rough surfaces and for polymer solutions which includes the smooth case is then applied to the circumferential velocity. The circumferential wall shearing stress is taken as the reference wall shearing stress instead of the resultant wall shearing stress as used by von Kármán and Goldstein. Certain inconsistencies are thus avoided. The actual difference in magnitude of these two wall shearing stresses is negligible. The radial velocity model used is that of Prandtl which is a generalization of the von Kármán model.

A general logarithmic formula is derived for the resisting moment of rotating disks which applies to arbitrary rough surfaces and/or drag-reducing polymer solutions. The special cases considered include:

1. Smooth surfaces.
2. Fully rough surfaces.
3. Polymer solutions with a linear logarithmic drag-reduction characterization.

5. Dorfman, L.A., "Drag of a Rotating Disk," Soviet Physics-Technical Physics, Vol. 3, No. 2, p. 353 (Feb 1958).

6. Dorfman, L.S., "Hydrodynamic Resistance and the Heat Loss of Rotating Solids," Oliver & Boyd, London (1963).

4. Maximum drag reduction with polymer solution.

Formulas are also derived for the local skin friction, the boundary-layer thickness, the displacement thickness, and the momentum thickness as functions of Reynolds number. In addition, solutions are obtained for the skewness of the boundary-layer velocity and for the skewness of the wall shearing stress. Comparisons are made with existing test data.

The appendix gives a generalization of the von Kármán power-law analysis for smooth disks which provides simple formulas for limited ranges of Reynolds number. The more accurate quadratic Mager model is used here for the radial velocity profile.

GENERAL ANALYSIS

MOMENTUM EQUATIONS

The steady-state equations of motion of turbulent flow in the neighborhood of a rotating disk⁴ are in cylindrical polar coordinates (see Figure 1) r , ϕ , and z with corresponding mean velocity components v_r , v_ϕ , and v_z . For the radial direction the equation is

$$v_r \frac{\partial v_r}{\partial r} + v_z \frac{\partial v_r}{\partial z} - \frac{v_\phi^2}{r} = \frac{1}{\rho r} \frac{\partial}{\partial r} (r p_{rr}) - \frac{p_{\phi\phi}}{\rho r} + \frac{1}{\rho} \frac{\partial p_{rz}}{\partial z} \quad (1)$$

and for the circumferential direction, it is

$$v_r \frac{\partial v_\phi}{\partial r} + v_z \frac{\partial v_\phi}{\partial z} + \frac{v_r v_\phi}{r} = \frac{1}{\rho r} \frac{\partial}{\partial r} (r p_{r\phi}) + \frac{p_{r\phi}}{\rho r} + \frac{1}{\rho} \frac{\partial p_{z\phi}}{\partial z} \quad (2)$$

where p_{rr} and $p_{\phi\phi}$ are the normal stress components;

p_{rz} , $p_{r\phi}$, and $p_{z\phi}$ are the shearing stress components; and

ρ is the density of the fluid.

The turbulent Reynolds stresses are included. The corresponding equation of continuity is

$$\frac{1}{r} \frac{\partial}{\partial r} (r v_r) + \frac{\partial v_z}{\partial z} = 0 \quad (3)$$

A three-dimensional boundary-layer flow exists next to the rotating disk with thickness δ . Integration of the equations of motion across the boundary layer and incorporation of the equations of continuity result in the von Kármán momentum equations⁴ for a rotating disk; in the radial direction, this is given by

$$\frac{d}{dr} \left(r \int_0^{\delta} v_r^2 dz \right) - \int_0^{\delta} v_{\phi}^2 dz = - r \frac{\tau_{w,r}}{\rho} \quad (4)$$

In the circumferential direction, it is given by

$$\frac{d}{dr} \left(r^2 \int_0^{\delta} v_r v_{\phi} dz \right) = - r^2 \frac{\tau'_{w,\phi}}{\rho} \quad (5)$$

von Kármán³ originally derived these equations from momentum considerations across flow control surfaces.

In Equations (4) and (5), $\tau_{w,r}$ is the radial component of the driving wall shearing stress and $\tau'_{w,\phi}$ is the circumferential component of the driving wall shearing stress. The boundary conditions for a disk rotating with angular velocity ω are $v_{\phi} = \omega r$ for $z = 0$ and $v_{\phi} = v_r = 0$ for $z = \delta$.

The momentum equations are changed to the usual form of boundary-layer momentum equations by considering the velocity relative to the rotating disk u in the circumferential direction

$$- u = v_{\phi} - r\omega \quad (6)$$

and the relative circumferential wall shearing stress $\tau_{w,\phi}$ is

$$\tau_{w,\phi} = - \tau'_{w,\phi} \quad (7)$$

Then the boundary conditions become $u = 0$ for $z = 0$ and $u = U = r\omega$ for $z = \delta$, and the momentum equations in boundary-layer form become

$$\omega^2 \frac{d}{dr} \left[r^3 \delta \int_0^{\delta} \left(\frac{v_r}{U} \right)^2 d \left(\frac{z}{\delta} \right) \right] - r^2 \omega^2 \delta \int_0^1 \left(1 - \frac{u}{U} \right)^2 d \left(\frac{z}{\delta} \right) = - r \frac{\tau_{w,r}}{\rho} \quad (8)$$

and

$$\omega^2 \frac{d}{dr} \left[r^4 \delta \int_0^1 \left(\frac{v_r}{U} \right) \left(\frac{v_\phi}{U} \right) d \left(\frac{z}{\delta} \right) \right] = r^2 \frac{\tau_{w,\phi}}{\rho} \quad (9)$$

RESISTING MOMENT OR TORQUE

The resisting moment or torque is given by

$$dM = \tau_{w,\phi} (2\pi r dr) r \quad (10)$$

or for the whole disk area on one side

$$M = 2\pi \int_0^r \tau_{w,\phi} r^2 dr \quad (11)$$

From the circumferential moment equation, Equation (9),

$$M = 2\pi \rho r^4 \omega^2 \delta \int_0^1 \left(\frac{v_r}{U} \right) \left(\frac{v_\phi}{U} \right) d \left(\frac{z}{\delta} \right) \quad (12)$$

A dimensionless moment coefficient k_m is defined by von Kármán³ for both sides of the disk as

$$k_m \equiv \frac{2M}{\rho r^5 \omega^2} = \frac{4\pi\delta}{r} \int_0^1 \left(\frac{v_r}{U} \right) \left(\frac{v_\phi}{U} \right) d \left(\frac{z}{\delta} \right) \quad (13)$$

A frequently used alternate moment coefficient C_m is defined as

$$C_m \equiv \frac{2M}{\frac{1}{2} \rho r^5 \omega^2} \quad (14)$$

or

$$C_m = 2 k_m \quad (15)$$

CIRCUMFERENTIAL VELOCITY PROFILE

The circumferential flow relative to the disk u , i.e., the relative streamwise flow, is assumed to obey similarity laws like that of pipe flow

and of boundary-layer flow on flat plates.^{1,2} There is no streamwise pressure gradient for the disk flow here. In analyses of three-dimensional turbulent boundary layers, the streamwise flow in the boundary layer is considered as a two-dimensional flow.

The inner similarity law for all cases including rough surfaces and polymer solutions is given by

$$\frac{u}{u_{\tau,\phi}} = f \left[\frac{u_{\tau,\phi} z}{\nu}, \ell^*, \dots \right] \quad (16)$$

where $\ell^* \equiv (u_{\tau,\phi} \ell / \nu)$ and ℓ is a characteristic length scale of roughness or polymer. The outer similarity law is

$$\frac{U - u}{u_{\tau,\phi}} = F \left[\frac{z}{\delta} \right] \quad (17)$$

where $u_{\tau,\phi} = \sqrt{\tau_{w,\phi} / \rho}$ is the tangential shear velocity and $\nu \equiv \mu / \rho$ is the kinematic viscosity of the fluid.

The two similarity laws are considered to overlap so that it can easily be shown¹ that within the region of overlap, the inner law becomes

$$\frac{u}{u_{\tau,\phi}} = A \ln \frac{u_{\tau,\phi} z}{\nu} + B_1 [\ell^*, \dots] \quad (18)$$

and the outer law becomes

$$\frac{U - u}{u_{\tau,\phi}} = -A \ln \frac{z}{\delta} + B_2 \quad (19)$$

B_1 is a constant for smooth surfaces in ordinary fluids but, for rough surfaces and for polymer solutions, it varies with ℓ^* and other pertinent factors which are constant for a given situation.

Equations (18) and (19) produce

$$\sigma \equiv \frac{U}{u_{\tau,\phi}} = A \ln \frac{u_{\tau,\phi} \delta}{\nu} + B_1 [\ell^*, \dots] + B_2 \quad (20)$$

or

$$\sigma = A \ln \frac{r\omega\delta}{\sigma v} + B_1 [\ell^* , \dots] + B_2 \quad (21)$$

The outer law encompasses almost all the boundary layer.¹ Accordingly, for considerations of momentum changes, the outer law is assumed to hold all the way to the wall, i.e., $0 < z/\delta < 1$. Then

$$\frac{v_\phi}{U} = 1 - \frac{u}{U} = \frac{1}{\sigma} F \left[\frac{z}{\delta} \right] \quad (22)$$

Also

$$\int_0^1 \left(\frac{v_\phi}{U} \right)^2 d \left(\frac{z}{\delta} \right) = \frac{\tilde{F}^2}{\sigma^2} \quad (23)$$

where

$$\tilde{F}^2 \equiv \int_0^1 F^2 d \left(\frac{z}{\delta} \right), \text{ a constant} \quad (24)$$

RADIAL VELOCITY PROFILE

The radial velocity profile v_r represents the cross-flow velocity component of three-dimensional boundary layers. Prandtl⁷ suggests a cross-flow velocity profile of form

$$\frac{v_r}{U} = \alpha \frac{u}{U} g \left[\frac{z}{\delta} \right] \quad (25)$$

where $g[1] = 0$ and $\alpha \equiv \tau_{w,r}/\tau_{w,\phi}$, the tangent of the angle of the resultant wall shearing stress from the circumferential direction. Von Kármán³ had already implicitly used this form for the disk with

7. Prandtl, L., "On Boundary Layers in Three-Dimensional Flow," B.I.G.S. 84 (Aug 1946); also British M.A.P. Report and Translation 64 (May 1946).

$$g \left[\frac{z}{\delta} \right] = 1 - \frac{z}{\delta} \quad (26)$$

as the simplest relation that satisfies boundary conditions. For cross flows in general, Mager⁸ finds a good fit to experimental data by

$$g \left[\frac{z}{\delta} \right] = \left(1 - \frac{z}{\delta} \right)^2 \quad (27)$$

Of course a $g[z/\delta]$ may be selected for rotating disks that conforms exactly to the experimental findings. Other forms of cross-flow velocity profiles are the triangular relations of Johnston⁹ and the polynomial relations of Eichelbrenner.¹⁰

Goldstein⁴ assumes somewhat arbitrarily a radial velocity profile of the form

$$\frac{v_r}{U} = \alpha \frac{u}{U} \left(\frac{U}{u} - 1 \right) \quad (28)$$

everywhere except close to the disk; for the remaining distance close to the disk wall, he assumes

$$\frac{v_r}{U} = \alpha \frac{u}{U} \quad (29)$$

8. Mager, A., "Generalization of Boundary Layer Momentum-Integral Equations to Three-Dimensional Flows Including Those of Rotating Systems," National Advisory Committee for Aeronautics Technical Report 1067 (1952).

9. Johnston, J.P., "On the Three-Dimensional Turbulent Boundary Layer Generated by Secondary Flow," Transactions of American Society of Mechanical Engineers, Journal of Basic Engineering, Vol. 82, Series D, No. 1 (Mar 1960).

10. Eichelbrenner, E.A., "La Couche Limite Tridimensionnelle en Régime Turbulent d'un Fluide Compressible," NATO Advisory Group for Aerospace Research AGARDograph 97 (May 1965).

SOLUTION OF MOMENTUM EQUATIONS

From the relation for boundary-layer thickness δ , Equation (21), and since by definition

$$\frac{\tau_{w,\phi}}{\rho} \equiv \frac{U^2}{\sigma^2} = \frac{r^2 \omega^2}{\sigma^2} \quad (30)$$

and

$$\frac{\tau_{w,r}}{\rho} \equiv \alpha \frac{\tau_{w,\phi}}{\rho} \quad (31)$$

the momentum equations, (8) and (9), become for the radial direction

$$\frac{d}{d\sigma} \left[\text{Re} \frac{\sigma^{-B_1-B_2}}{A} \sigma \int_0^1 \left(\frac{v_r}{U} \right)^2 d \left(\frac{z}{\delta} \right) \right] = \frac{1}{2} \left[e \frac{\sigma^{-B_1-B_2}}{A} \sigma \int_0^1 \left(\frac{v_\phi}{U} \right)^2 d \left(\frac{z}{\delta} \right) - \frac{\alpha R}{\sigma^2} \right] \frac{dR}{d\sigma} \quad (32)$$

and for the circumferential direction

$$\frac{d}{d\sigma} \left[R^{3/2} e \frac{\sigma^{-B_1-B_2}}{A} \sigma \int_0^1 \left(\frac{v_r}{U} \right) \left(\frac{v_\phi}{U} \right) d \left(\frac{z}{\delta} \right) \right] = \frac{1}{2} \frac{R^{3/2}}{\sigma^2} \frac{dR}{d\sigma} \quad (33)$$

The Reynolds number R is defined as

$$R \equiv \frac{\omega r^2}{\nu} \quad (34)$$

A clue to the form of the solution to the circumferential momentum Equation, (33), namely $R[\sigma]$, is indicated as follows. If Equation (33) is rewritten as

$$\sigma^2 \frac{d}{dR} \left[R^{3/2} e \frac{\sigma^{-B_1-B_2}}{A} \sigma \int_0^1 \left(\frac{v_r}{U} \right) \left(\frac{v_\phi}{U} \right) d \left(\frac{z}{\delta} \right) \right] = \frac{1}{2} R^{3/2} \quad (35)$$

an integration by parts from $R = 0$ to $R = R$ results in

$$R = 5e \frac{\sigma - B_1 - B_2}{A} \sigma^3 \int_0^1 \left(\frac{v_r}{U} \right) \left(\frac{v_\phi}{U} \right) d \left(\frac{z}{\delta} \right) - \frac{10}{R^{3/2}} \int_0^\sigma \left[R^{3/2} e^{-\frac{\sigma - B_1 - B_2}{A}} \sigma^2 \int_0^1 \left(\frac{v_r}{U} \right) \left(\frac{v_\phi}{U} \right) d \left(\frac{z}{\delta} \right) \right] d\sigma \quad (36)$$

For the Prandtl form of the radial velocity profile, from Equations (22) and (25),

$$\frac{v_r}{U} = \alpha g \left[\frac{z}{\delta} \right] \left(1 - \frac{1}{\sigma} F \left[\frac{z}{\delta} \right] \right) \quad (37)$$

the integrals of the velocity profiles required for Equations (32) and (33) become

$$\int_0^1 \left(\frac{v_r}{U} \right)^2 d \left(\frac{z}{\delta} \right) = \alpha^2 \tilde{g}^2 \left(1 - \frac{2h_2}{\sigma} + \frac{h_3}{\sigma^2} \right) \quad (38)$$

and

$$\int_0^1 \left(\frac{v_r}{U} \right) \left(\frac{v_\phi}{U} \right) d \left(\frac{z}{\delta} \right) = \frac{\alpha}{\sigma} \tilde{F} \tilde{g} \left(1 - \frac{h_1}{\sigma} \right) \quad (39)$$

where

$$h_1 = \tilde{F} \tilde{g}^2 / \tilde{F} \tilde{g} \quad (40)$$

$$h_2 = \tilde{F} \tilde{g}^2 / \tilde{g}^2 \quad (41)$$

$$h_3 = \tilde{F}^2 \tilde{g}^2 / \tilde{g}^2 \quad (42)$$

and in general

$$[\tilde{\quad}] = \int_0^1 [\quad] d \left(\frac{z}{\delta} \right) \quad (43)$$

are constants.

The momentum equations, (32) and (33), become for the radial direction

$$\tilde{g}^2 \frac{d}{d\sigma} \left[\alpha^2 R e^{\frac{\sigma-B_1-B_2}{A}} \sigma \left(1 - \frac{2h_2}{\sigma} + \frac{h_3}{\sigma^2} \right) \right] = \frac{1}{2} \left(\frac{\tilde{F}^2}{\sigma} e^{\frac{\sigma-B_1-B_2}{A}} - \frac{\alpha R}{\sigma^2} \right) \frac{dR}{d\sigma} \quad (44)$$

and for the circumferential direction

$$\tilde{F}g \frac{d}{d\sigma} \left[\alpha R^{3/2} e^{\frac{\sigma-B_1-B_2}{A}} \left(1 - \frac{h_1}{\sigma} \right) \right] = \frac{1}{2} \frac{R^{3/2}}{\sigma^2} \frac{dR}{d\sigma} \quad (45)$$

From the partial solution of the circumferential equation, (36),

$$R = 5\tilde{F}g \alpha \sigma^2 e^{\frac{\sigma-B_1-B_2}{A}} \left[1 - \frac{h_1}{\sigma} + \dots \right] \quad (46)$$

Hence let

$$R = \alpha \sigma^2 e^{\frac{\sigma-B_1-B_2}{A}} \beta[\sigma] \quad (47)$$

where $\beta[\sigma]$ is to be determined as well as $\alpha[\sigma]$.

Prior to the solution of $R[\sigma]$, $\beta[\sigma]$, and $\alpha[\sigma]$, it is expedient to obtain some intermediate relationships. The factor B_1 is constant for smooth surfaces but $B_1[\ell^*, \dots]$ for rough surfaces and for disks in drag-reducing polymer solutions. Since, by definition, $\ell^* \equiv u_{\tau, \phi} \ell / \nu \equiv \ell \sqrt{\omega / \nu} R^{1/2} / \sigma$, then

$$\frac{dB_1[\ell^*]}{d\sigma} = B_1' \left(\frac{1}{2R} \frac{dR}{d\sigma} - \frac{1}{\sigma} \right) \quad (48)$$

where $B_1' \equiv dB_1/d[\ln \ell^*]$.

Likewise

$$\frac{dR}{d\sigma} = \frac{2\alpha\beta\sigma^2}{(2A + B_1')} e^{\frac{\sigma-B_1-B_2}{A}} \left[1 + \frac{(2A + B_1')}{\sigma} + A \left(\frac{\alpha'}{\alpha} + \frac{\beta'}{\beta} \right) \right] \quad (49)$$

where

$$\alpha' = \frac{d\alpha}{d\sigma} \text{ and } \beta' = \frac{d\beta}{d\sigma}$$

Hence

$$\frac{dB_1[\lambda^*]}{d\sigma} = \frac{B_1'}{(2A + B_1')} \left[1 + A \left(\frac{\alpha'}{\alpha} + \frac{\beta'}{\beta} \right) \right] \quad (50)$$

Also, in general,

$$\frac{d}{d\sigma} \left[e^{\left(m \frac{\sigma - B_1 - B_2}{A} \right)} \right] = \frac{2m}{2A + B_1'} e^{\left(m \frac{\sigma - B_1 - B_2}{A} \right)} \left[1 - \frac{B_1'}{2} \frac{\alpha'}{\alpha} + \frac{\beta'}{\beta} \right] \quad (51)$$

where m is a constant.

By using $R[\sigma]$, given in Equation (47), and performing the indicated operations, the circumferential momentum equation, (45), is reduced to

$$\begin{aligned} s\bar{F}g \left(1 - \frac{h_1}{\sigma} \right) & \left\{ 1 + \frac{(2A + B_1')}{5} \left[\frac{3}{\sigma} + \frac{h_1}{\sigma^2} \left(\frac{h_1}{1 - \frac{h_1}{\sigma}} \right) \right] + A \frac{\alpha'}{\alpha} + \frac{\beta'}{5\beta} (3A - B_1') \right\} \\ & = \beta \left[1 + \frac{2A + B_1'}{\sigma} + A \left(\frac{\alpha'}{\alpha} + \frac{\beta'}{\beta} \right) \right] \end{aligned} \quad (52)$$

The radial momentum equation, (44), is reduced to

$$\begin{aligned} 2\bar{g}^2 \alpha^2 \sigma^2 \left(1 - \frac{2h_2}{\sigma} + \frac{h_3}{\sigma^2} \right) & \left[1 - \frac{B_1'}{2} \left(\frac{\alpha'}{\alpha} + \frac{\beta'}{\beta} \right) + \frac{(2A + B_1')}{4} \frac{\lambda'}{\lambda} + \frac{2A + B_1'}{2\sigma} \right] \\ & = \left(\frac{\bar{F}^2 - \alpha^2 \beta \sigma}{2} \right) \left[1 + \frac{2A + B_1'}{\sigma} + A \left(\frac{\alpha'}{\alpha} + \frac{\beta'}{\beta} \right) \right] \end{aligned} \quad (53)$$

where

$$\lambda = \alpha^3 \beta \sigma \left(1 - \frac{2h_2}{\sigma} + \frac{h_3}{\sigma^2} \right) \quad (54)$$

and

$$\lambda' \equiv \frac{d\lambda}{d\sigma}$$

Let

$$\beta = b_0 \left(1 + \frac{b_1}{\sigma} + \frac{b_2}{\sigma^2} + \dots \right) \quad (55)$$

and

$$\alpha = \frac{a_0}{\sigma} \left(1 + \frac{a_1}{\sigma} + \frac{a_2}{\sigma^2} + \dots \right) \quad (56)$$

Substitution of the relations for α and β into the reduced momentum equations, (52) and (53), and equating coefficients in like powers of $1/\sigma$ produces

$$\begin{aligned} a_0 &= \frac{1}{2} \sqrt{\frac{\tilde{F}^2}{g}} \\ a_1 &= \frac{1}{2} (2A + B'_1) - \frac{h_2}{8} \\ b_0 &= 5 \tilde{F}g \\ b_1 &= -\frac{2}{5} (2A + B'_1) - h_1 \\ b_2 &= \frac{2}{5} (2A + B'_1) \left(h_1 + \frac{3A + 4B'_1}{5} \right) \end{aligned} \quad (57)$$

and so on.

LOGARITHMIC MOMENT FORMULAS

GENERAL

With the insertion of the relation for δ from Equation (21), the relation for the moment coefficient, Equation (13), becomes

$$k_m = \frac{4\pi}{R} \sigma e^{\frac{\sigma - B_1 - B_2}{A}} \int_0^1 \left(\frac{v_r}{U}\right) \left(\frac{v_\phi}{U}\right) d\left(\frac{z}{\delta}\right) \quad (58)$$

Using the relations for the radial velocity profile and the appropriate solution, $R[\sigma]$, gives $k_m[\sigma]$; k_m is then related to Reynolds number R implicitly through parameter σ . However, σ may be eliminated and k_m related to R in logarithmic formulas to follow.

By inserting the velocity profile integral, Equation (39), and the expression for R , Equation (47), the overall force coefficient k_m in Equation (13) is related to the local force coefficient σ as

$$k_m = \frac{4\pi \tilde{F}g}{\sigma^2 \beta} \left(1 - \frac{h_1}{\sigma}\right) \quad (59)$$

More explicitly with β given by the $\frac{1}{\sigma}$ series, Equation (55), and b_0 by Equation (57)

$$k_m = \frac{4\pi}{5} \frac{1}{\sigma^2} \left[1 - \frac{(b_1 + h_1)}{\sigma} + \frac{b_1(b_1 + h_1) - b_2}{\sigma^2} + \dots\right] \quad (60)$$

or

$$\sigma^2 = \frac{4\pi}{5} \frac{1}{k_m} \left[1 - \frac{(b_1 + h_1)}{\sigma} + \frac{b_1(b_1 + h_1) - b_2}{\sigma^2} + \dots\right] \quad (61)$$

By reiteration, the σ 's within the brackets are replaced by k_m 's such that

$$\sigma^2 = \frac{4\pi}{5} \frac{1}{k_m} \left[1 - (b_1 + h_1) \sqrt{\frac{5}{4\pi}} \sqrt{k_m} - \left(b_2 - \frac{b_1^2}{2} + \frac{h_1^2}{2}\right) \frac{5}{4\pi} \sqrt{k_m^2} + \dots\right] \quad (62)$$

or by binomial expansion

$$\sigma = \sqrt{\frac{4\pi}{5}} \frac{1}{\sqrt{k_m}} \left[1 - \frac{(b_1 + h_1)}{2} \sqrt{\frac{5}{4\pi}} \sqrt{k_m} - \frac{1}{8} (4b_2 - b_1^2 + 2b_1 h_1 + 3h_1^2) \frac{5}{4\pi} \sqrt{k_m^2} + \dots\right] \quad (63)$$

and

$$\frac{1}{\sigma} = \sqrt{\frac{5}{4\pi}} \sqrt{k_m} \left[1 + \frac{(b_1 + h_1)}{2} \sqrt{\frac{5}{4\pi}} \sqrt{k_m} + \dots \right] \quad (64)$$

Inserting the velocity profile integral, Equations (39) and (21), into the moment equation, (13), yields

$$k_m = \frac{4\pi}{R} \alpha e^{\frac{\sigma - B_1 - B_2}{A}} \tilde{F}g \left(1 - \frac{h_1}{\sigma} \right) \quad (65)$$

Substituting for α by Equation (56) and taking the natural logarithm results in

$$\ln k_m = \ln 4\pi - \ln R + \frac{\sigma}{A} - \frac{B_1}{A} - \frac{B_2}{A} + \ln a_o - \ln \sigma - \frac{a_1}{\sigma} + \ln \tilde{F}g - \frac{h_1}{\sigma} + \dots \quad (66)$$

Eliminating the σ 's through Equations (62) to (64) gives, in general,

$$\begin{aligned} \frac{1}{\sqrt{k_m}} = & A \sqrt{\frac{5}{4\pi}} \ln R \sqrt{k_m} + \sqrt{\frac{5}{4\pi}} (B_1 + B_2) - \frac{A}{\sqrt{5\pi}} - \frac{B'_1}{\sqrt{20\pi}} - A \sqrt{\frac{5}{4\pi}} \ln \left(\tilde{F}g \sqrt{\frac{5\pi \tilde{F}^2}{g^2}} \right) \\ & - \frac{5A}{4\pi} \left[-\frac{1}{8A} (4b_2 - b_1^2 + 2b_1h_1 + 3h_1^2) + \frac{b_1}{2} + a_1 - \frac{h_1}{2} \right] \sqrt{k_m} + \dots \quad (67) \end{aligned}$$

SMOOTH SURFACES IN ORDINARY FLUIDS

Throughout the report, these are termed the smooth case.

Here $B'_1 = 0$, and the logarithmic moment law becomes in common logarithms

$$\begin{aligned} \frac{1}{\sqrt{k_m}} = & A_1 \sqrt{\frac{5}{4\pi}} \log R \sqrt{k_m} + \sqrt{\frac{5}{4\pi}} (B_{1,0} + B_2) - \frac{A}{\sqrt{5\pi}} \\ & - A_1 \sqrt{\frac{5}{4\pi}} \log \left(\tilde{F}g \sqrt{\frac{5\pi \tilde{F}^2}{g^2}} \right) + D \sqrt{k_m} + \dots \quad (68) \end{aligned}$$

where $A_1 = 2.3026 A$

and

$$D = \frac{5}{4\pi} A \left(h_1 + \frac{h_2}{8} - \frac{11}{25} A \right) \quad (69)$$

If $\sqrt{k_m}$ is linearized with respect to $1/\sqrt{k_m}$ as

$$\sqrt{k_m} \approx c_1 + \frac{c_2}{\sqrt{k_m}} \quad (70)$$

and terms of order higher than $\sqrt{k_m}$ are neglected, then

$$\frac{1}{\sqrt{k_m}} = A \log R \sqrt{k_m} + B \quad (71)$$

where

$$A = \frac{A_1 \sqrt{\frac{5}{4\pi}}}{1 - c_2 D} \quad (72)$$

and

$$B = \frac{1}{(1 - c_2 D)} \left[\sqrt{\frac{5}{4\pi}} (B_{1,0} + B_2) - \frac{A}{\sqrt{5\pi}} - A_1 \sqrt{\frac{5}{4\pi}} \log \left(\tilde{F} g \sqrt{\frac{5\pi}{g^2} \tilde{F}^2} \right) + c_1 D \right] \quad (73)$$

Equation (71) is the same general form for the logarithmic moment law as obtained by Goldstein.⁴

ROUGH SURFACES OR DRAG-REDUCING POLYMER SOLUTIONS

Ignoring the negligible effects of B'_1 in the coefficients such as b_1 and b_2 before $\sqrt{k_m}$ in Equation (67) (see Equation (57)) provides a logarithmic moment law for rough surfaces and for disks in drag-reducing polymer solutions

$$\frac{1}{\sqrt{k_m}} = A \log R \sqrt{k_m} + B + \frac{1}{(1 - c_2 D)} \left[\sqrt{\frac{5}{4\pi}} (B_1 - B_{1,0}) - \frac{B'_1}{\sqrt{20\pi}} \right] \quad (74)$$

where $B_{1,0} = B_1$ for smooth surfaces in ordinary fluids.

SPECIAL LOGARITHMIC MOMENT FORMULAS

FULLY ROUGH SURFACES

For fully rough surfaces¹

$$B_1 = B_3 - A \ln \ell^* = B_3 - A \ln k^* \quad (75)$$

where B_3 is a constant. Here $\ell = k$, the roughness length scale. Then $B_1' = -A$.

Since by definition

$$k^* \equiv \frac{1}{\sigma} R \frac{k}{r} \quad (76)$$

$$B_1 = B_3 + A_1 \log \sigma - A_1 \log R + A_1 \log \frac{r}{k} \quad (77)$$

From Equation (63)

$$\log \sigma = \log \sqrt{\frac{4\pi}{5}} - \log \sqrt{k_m} + \frac{1}{5} \frac{(2A + B_1')}{2.3026} \sqrt{\frac{5}{4\pi}} \sqrt{k_m} + \dots \quad (78)$$

Then from Equation (67)

$$\frac{1}{\sqrt{k_m}} = A_1 \log \frac{r}{k} + B_1 \quad (79)$$

$$k_m = \frac{1}{(A_1 \log \frac{r}{k} + B_1)^2} \quad (80)$$

where

$$A_1 = \frac{\sqrt{\frac{5}{4\pi}} A_1}{1 + \frac{c_2 5A}{4\pi} \left(\frac{11}{50} A - h_1 - \frac{h_2}{8} \right)} \quad (81)$$

and

$$B_1 = \frac{\sqrt{\frac{5}{4\pi}}}{1 + \frac{c_2 5A}{4\pi} \left(\frac{11}{50} A - h_1 - \frac{h_2}{8} \right)} \left[B_3 + B_2 - \frac{A}{5} + A_1 \log \sqrt{\frac{4\pi}{5}} - A_1 \log \left(\tilde{F}_g \sqrt{\frac{5\pi \tilde{F}_g^2}{g^2}} \right) - c_1 \sqrt{\frac{5}{4\pi}} A \left(\frac{11}{50} A - h_1 - \frac{h_2}{8} \right) \right] \quad (82)$$

ENGINEERING ROUGHNESS

For surfaces with engineering roughness (Colebrook-White roughness)¹

$$B_1 = B_{1,0} - A \ln \left(1 + \frac{k^*}{p} \right) \quad (83)$$

where

$$p = e^{\frac{B_2 - B_{1,0}}{A}} \quad (84)$$

Then

$$B'_1 = - \frac{A}{1 + \frac{p}{k^*}} \quad (85)$$

From Equation (76) and Equation (64),

$$1 + \frac{k^*}{p} = 1 + \frac{1}{p} \left(\frac{1}{\sigma} R \frac{k}{r} \right) = \left(\frac{1}{R \sqrt{k_m}} + \frac{1}{p} \sqrt{\frac{5}{4\pi}} \frac{k}{r} \right) R \sqrt{k_m} + \dots \quad (86)$$

Likewise

$$B'_1 = - \frac{A}{p \sqrt{\frac{4\pi}{3}} \frac{r}{k} \left(\frac{1}{R \sqrt{k_m}} + \frac{1}{p \sqrt{\frac{4\pi}{3}} \frac{r}{k}} \right)} + \dots \quad (87)$$

Substituting into Equation (67) produces

$$-A \log \left(\frac{1}{R\sqrt{k_m}} + \frac{1}{p\sqrt{\frac{4\pi}{5} \frac{r}{k}}} \right) = \frac{1}{\sqrt{k_m}} - B - \frac{1}{2.3026 p \sqrt{20\pi} \frac{r}{k}} \left(\frac{1}{R\sqrt{k_m}} + \frac{1}{p\sqrt{\frac{4\pi}{5} \frac{r}{k}}} \right), \quad (88)$$

For $r/k \rightarrow \infty$, Equation (88) reduces to the moment formula for smooth surfaces; for $R\sqrt{k_m} \rightarrow \infty$, Equation (88) reduces to the moment formula for fully rough surfaces.

POLYMER SOLUTIONS WITH LINEAR LOGARITHMIC CHARACTERIZATION*

It has been found experimentally that for some polymer solutions² B_1 is a linear logarithmic function of l^* . Then

$$B_1 = B_{1,0} - A_1 \log \frac{\nu_s}{\nu} + q(\log l^* - \log l_0^*), \quad l^* > l_0^* \quad (89)$$

$$B_1 = B_{1,0} - A_1 \log \frac{\nu_s}{\nu}, \quad l^* < l_0^*$$

where $B_{1,0}$ is a constant,

ν_s is the kinematic viscosity of the solution,

ν is the kinematic viscosity of the solvent,

l_0^* is the drag-reduction threshold value of l^* , and

$B_1^! = dB_1/2.3d (\log l^*) = q/2.3$.

Since from Equation (76) and Equation (64),

$$l^* = \frac{1}{\sigma} R \frac{\ell}{r} = R \frac{\ell}{r} \sqrt{\frac{5}{4\pi}} \sqrt{k_m} \left[1 - \frac{(2A + B_1^!)}{\sqrt{20\pi}} \sqrt{k_m} + \dots \right] \quad (90)$$

* After the present report was written, Poreh and Miloh extended the Goldstein analytical model to this case ("Rotation of a Disk in Dilute Polymer Solutions," Journal of Hydronautics, Vol. 5, No. 2, Apr 1971).

then

$$B_1 - B_{1,0} = -A_1 \log \frac{v_s}{v} + q \left[\log R \sqrt{k_m} - \log \frac{r}{\ell} + \log \sqrt{\frac{5}{4\pi}} - \left(2A + \frac{q}{2.3} \right) \frac{\sqrt{k_m}}{\sqrt{20\pi}} - \log \ell_o^* + \dots \right] \quad (91)$$

Finally

$$\frac{1}{\sqrt{k_m}} = A_2 \log R \sqrt{k_m} + B_2 - \frac{\sqrt{\frac{5}{4\pi}}}{1-c_2} D q \log \frac{r}{\ell} \quad (92)$$

where

$$A_2 = A + \frac{\sqrt{\frac{5}{4\pi}}}{1-c_2} D q \quad (93)$$

and

$$B_2 = B + \frac{\sqrt{\frac{5}{4\pi}}}{1-c_2} D \left[-A_1 \log \frac{v_s}{v} + q \log \sqrt{\frac{5}{4\pi}} - \frac{q}{5(2.3026)} - q \log \ell_o^* \right] \quad (94)$$

The onset of drag reduction is given by $\ell^* = \ell_o^*$. If ℓ is chosen so $\ell_o^* = 1$, then from Equation (90), the onset of drag reduction occurs when

$$\sqrt{\frac{5}{4\pi}} R \sqrt{k_m} \frac{\ell}{r} \left[1 - \frac{(2A_1+q)}{2.3 \sqrt{20\pi}} \sqrt{k_m} \right] = 1 \quad (95)$$

SURFACE WITH LAMINAR AND TURBULENT FLOW

For laminar flow⁶

$$k_m = \frac{1.935}{R^{1/2}} \quad (96)$$

Physically, the flow in the boundary layer is laminar starting from the center of the disk at $r = 0$ and undergoes transition to turbulent flow at $r = r_t$ specified by a Reynolds number of transition R_t .

Although the logarithmic moment formulas are derived for complete turbulent flow over the disk, a correction may be made for the presence of

laminar flow in the central part of the disk. The correction is required only for an intermediate range of Reynolds numbers.

The moment of the area up to transition is subtracted for the turbulent flow and added on for the laminar flow. Then the corrected k_m for the disk with partial laminar flow becomes simply

$$k_m = (k_m)_{\text{turb}} - \left(\frac{R_t}{R}\right)^{5/2} \left[(k_{m,t})_{\text{turb}} - (k_{m,t})_{\text{lam}} \right] \quad (97)$$

Obviously the correction becomes smaller for increasing R . $R_t = 2.9 \times 10^5$ has been observed for smooth surfaces.¹¹

LOCAL SKIN FRICTION

The components of the local skin friction or wall shearing stress $\tau_{w,\phi}$ and $\tau_{w,r}$ are expressed in terms of parameter σ by Equations (30) and (31); σ may be obtained as function of Reynolds number R as follows:

Substitution of α and β from Equations (56) and (55) in the relation for R , Equation (47), produces

$$R = a_o b_o \sigma e^{\frac{\sigma - B_1 - B_2}{A}} \left(1 + \frac{a_1 + b_1}{\sigma} + \frac{a_2 + a_1 b_1 + b_2}{\sigma^2} + \dots \right) \quad (98)$$

To obtain a more compact although slightly more approximate relation, the logarithm is taken and terms of order $1/\sigma$ and higher are dropped so that

$$\sigma = A_1 \log R - A_1 \log a_o b_o + B_1 + B_2 - A_1 \log \sigma - \frac{A(a_1 + b_1)}{\sigma} + \dots \quad (99)$$

11. Gregory, N. et al., "On the Stability of Three-Dimensional Boundary Layers with Application to the Flow Due to a Rotating Disk," *Philosophical Transactions of Royal Society, London (A)* 248, p. 155 (1955); also in "Boundary Layer Effects in Aerodynamics," Symposium at National Physical Laboratory, Great Britain (1955); published by Philosophical Library, New York (1957).

If $\log \sigma \approx c_3 + c_4 \sigma$ (100)

and

$$\frac{1}{\sigma} \approx c_5 + c_6 \sigma \quad (101)$$

then

$$\sigma = p_1 \log R + p_2 \quad (102)$$

where

$$p_1 = \frac{A_1}{1 + c_4 A_1 + c_6 A(a_1 + b_1)} \quad (103)$$

and

$$p_2 = \frac{B_1 + B_2 - A_1 \left[\log \frac{a}{o} \frac{b}{o} + c_3 + \frac{c_5}{2.3026} (a_1 + b_1) \right]}{1 + c_4 A_1 + c_6 A(a_1 + b_1)} \quad (104)$$

For the smooth case (ordinary fluids), p_1 and p_2 are constants.

Also for a coefficient of local skin friction C_f where $C_f \equiv \tau_{w,\phi} / \frac{1}{2} \rho U^2$,

$$C_f = \frac{2}{\sigma^2} = \frac{2}{(p_1 \log R + p_2)^2} \quad (105)$$

BOUNDARY-LAYER THICKNESSES

ORDINARY BOUNDARY-LAYER THICKNESS

From Equation (21), the ordinary boundary-layer thickness δ is given by

$$\delta = \frac{\nu \sigma}{r \omega} e^{\frac{\sigma - B_1 - B_2}{A}} \quad (106)$$

and nondimensionally by

$$\delta \sqrt{\frac{\omega}{\nu}} = \frac{\sigma}{\sqrt{R}} e^{\frac{\sigma - B_1 - B_2}{A}} \quad (107)$$

or

$$\frac{\delta}{R} = \frac{\sigma}{R} e^{\frac{\sigma - B_1 - B_2}{A}} \quad (108)$$

To obtain $\delta \sqrt{\frac{\omega}{\nu}}$ as a function of Reynolds number R , the common logarithm of Equation (107) produces

$$\log \delta \sqrt{\frac{\omega}{\nu}} = \log \sigma - \frac{1}{2} \log R + \frac{\sigma}{A_1} - \frac{B_1}{A_1} - \frac{B_2}{A_1} \quad (109)$$

The $\log \sigma$ and σ are converted to functions of R through Equations (100) and (102).

Then

$$\begin{aligned} \log \delta \sqrt{\frac{\omega}{\nu}} = & \left[p_1 \left(\frac{1}{A_1} + c_4 \right) - \frac{1}{2} \right] \log R \\ & + \left[\left(\frac{1}{A_1} + c_4 \right) p_2 + c_3 - \frac{B_1}{A_1} - \frac{B_2}{A_1} \right] \end{aligned} \quad (110)$$

or

$$\delta \sqrt{\frac{\omega}{\nu}} = s_1 R^{s_2} \quad (111)$$

where

$$\log s_1 = \left(\frac{1}{A_1} + c_4 \right) p_2 + c_3 - \frac{B_1}{A_1} - \frac{B_2}{A_1} \quad (112)$$

and

$$s_2 = p_1 \left(\frac{1}{A_1} + c_4 \right) - \frac{1}{2} \quad (113)$$

Also

$$\frac{\delta}{R} = s_1 R^{s_2 - \frac{1}{2}} \quad (114)$$

DISPLACEMENT THICKNESS

From the usual definition of displacement thickness,

$$\delta^* \equiv \int_0^{\delta} \left(1 - \frac{u}{U}\right) dz \quad (115)$$

Then

$$\frac{\delta^*}{\delta} = \frac{\tilde{F}}{\sigma} \quad (116)$$

where

$$\tilde{F} \equiv \int_0^1 F d\left(\frac{z}{\delta}\right) \quad (117)$$

From Equation (107),

$$\delta^* \sqrt{\frac{\omega}{\nu}} = \frac{\tilde{F}}{\sqrt{R}} e^{\frac{\sigma - B_1 - B_2}{A}} \quad (118)$$

and from Equation (108),

$$\frac{\delta^*}{r} = \frac{\tilde{F}}{R} e^{\frac{\sigma - B_1 - B_2}{A}} \quad (119)$$

To obtain $\delta^* \sqrt{\frac{\omega}{\nu}}$ as a function of R , the logarithm is taken so that

$$\log \delta^* \sqrt{\frac{\omega}{\nu}} = \log \tilde{F} - \frac{1}{2} \log R + \frac{\sigma}{A_1} - \frac{B_1}{A_1} - \frac{B_2}{A_2} \quad (120)$$

The elimination of σ by means of Equation (102) produces

$$\log \delta^* \sqrt{\frac{\omega}{\nu}} = \left(\frac{P_1}{A_1} - \frac{1}{2}\right) \log R + \log \tilde{F} + \frac{P_2}{A_1} - \frac{B_1}{A_1} - \frac{B_2}{A_1} \quad (121)$$

or

$$\delta^* \sqrt{\frac{\omega}{\nu}} s_3 R^{s_4} \quad (122)$$

where

$$\log s_3 = \log \tilde{F} + \frac{1}{A_1} (p_2 - B_1 - B_2) \quad (123)$$

and

$$s_4 = \frac{P_1}{A_1} - \frac{1}{2} \quad (124)$$

Also

$$\frac{\delta^*}{r} = s_3 R^{s_4 - \frac{1}{2}} \quad (125)$$

MOMENTUM THICKNESS

From the usual definition of momentum thickness,

$$\theta \equiv \int_0^{\delta} \frac{u}{U} \left(1 - \frac{u}{U}\right) dz \quad (126)$$

Then

$$\frac{\theta}{\delta} = \frac{\tilde{F}}{\sigma} - \frac{\tilde{F}^2}{\sigma^2} \quad (127)$$

From Equation (107),

$$\theta \sqrt{\frac{\omega}{\nu}} = \frac{1}{\sqrt{R}} e^{\frac{\sigma - B_1 - B_2}{A}} \left(\tilde{F} - \frac{\tilde{F}^2}{\sigma} \right) \quad (128)$$

or

$$\theta \sqrt{\frac{\omega}{\nu}} = \delta^* \sqrt{\frac{\omega}{\nu}} - \theta_1 \sqrt{\frac{\omega}{\nu}} \quad (129)$$

where

$$\theta_1 \sqrt{\frac{J}{V}} \equiv \frac{1}{\sqrt{R}} \bar{F}^2 e^{\frac{\sigma - B_1 - B_2}{A}} \quad (130)$$

Then as before,

$$\theta_1 \sqrt{\frac{\omega}{V}} = s_5 R^{s_6} \quad (131)$$

where

$$\log s_5 = \log \bar{F}^2 - c_3 - \frac{B_1}{A_1} - \frac{B_2}{A_1} + p_2 \left(\frac{1}{A_1} - c_4 \right) \quad (132)$$

and

$$s_6 = p_1 \left(\frac{1}{A_1} - c_4 \right) - \frac{1}{2} \quad (133)$$

Finally,

$$\theta \sqrt{\frac{\omega}{V}} = s_3 R^{s_4} - s_5 R^{s_6} \quad (134)$$

SHAPE PARAMETER

The usual definition of shape parameter H is

$$H \equiv \frac{\delta^*}{\theta} \quad (135)$$

Then from Equations (125) and (134),

$$H = \frac{1}{1 - \frac{s_5}{s_3} R^{s_6 - s_4}} \quad (136)$$

or

$$1 - \frac{1}{H} = \frac{s_5}{s_3} R^{s_6 - s_4} \quad (137)$$

COMPARISONS WITH EXPERIMENTAL DATA

EVALUATION OF VELOCITY INTEGRALS

Numerical values are required for the various velocity integrals designated in the formulas derived in this report. These may be obtained directly from experimental data or be evaluated indirectly from analytical models as follows:

1. For the circumferential velocity, Equation (17),

$$F = -A \ln \eta + B_2 \left(1 - \frac{w}{2}\right) \quad (138)$$

Here $\eta \equiv z/\delta$ and w is the Coles¹² wake function which is given a polynomial fit by Moses¹³ as

$$\frac{w}{2} = 3\eta^2 - 2\eta^3 \quad (139)$$

2. For the radial velocity, Equation (25), the Mager relation is used:

$$g = (1-\eta)^2$$

The various integrals then become

$$\tilde{F}g = \frac{1}{3} \frac{11}{6} A + \frac{4}{5} B_2 \quad (140)$$

$$\tilde{F}g^2 = \frac{1}{9} \frac{85}{6} A^2 + \frac{274}{25} A B_2 + \frac{29}{14} B_2^2 \quad (141)$$

$$\tilde{F}g^2 = \frac{137}{300} A - \frac{73}{140} B_2 \quad (142)$$

$$\tilde{g}^2 = \frac{1}{5} \quad (143)$$

12. Coles, D., "The Law of the Wake in the Turbulent Boundary Layer," *Journal of Fluid Mechanics*, Vol. 1, Pt. 2 (Jul 1956).

13. Moses, H.L., "The Behavior of Turbulent Boundary Layers in Adverse Pressure Gradients," Massachusetts Institute of Technology Gas Turbine Laboratory Report 73 (Jan 1964).

$$\bar{F}^2 = 2 A^2 + \frac{19}{12} A B_2 + \frac{13}{35} B_2^2 \quad (144)$$

$$\bar{F} = A + \frac{B_2}{2} \quad (145)$$

Then

$$h_1 = \frac{\bar{F}g^2}{\bar{F}g} = \frac{\frac{85}{6} A^2 + \frac{274}{25} A B_2 + \frac{29}{14} B_2^2}{3 \left(\frac{11}{6} A + \frac{4}{5} B_2 \right)} \quad (146)$$

$$h_2 = \frac{137}{60} A - \frac{73}{28} B_2 \quad (147)$$

SOURCES OF EXPERIMENTAL DATA

An account of early resistance experiments with rotating disks is given by Dryden et al.¹⁴ Data for higher Reynolds numbers and for smooth and rough surfaces are presented by Theodorsen and Regier.¹⁵ Resistance measurement with polymer solutions are reported by Hoyt and Fabula,¹⁶ by

14. Dryden, J.L. et al., "Hydrodynamics," National Research Council Bulletin 84 (1932); reprinted by Dover Publications, New York, p. 352 (1956).

15. Theodorsen, T. and A. Regier, "Experiments on Drag of Revolving Disks, Cylinders and Streamline Rods at High Speeds," National Advisory Committee for Aeronautics Technical Report 793 (1944).

16. Hoyt, J.W. and A.G. Fabula, "The Effect of Additives on Fluid Friction," 5th Symposium on Naval Hydrodynamics, Office of Naval Research ACR-112, U.S. Government Printing Office, Washington, D.C. (Sep 1964).

Amfilokhiev and Ferguson,¹⁷ and by Smallman and Wade.¹⁸ Velocity surveys have been performed by Gregory et al.,¹¹ by Stain,¹⁹ by Gadd,²⁰ by Cham and Head,²¹ and by Erian.²²

VELOCITY PROFILES

For the *smooth case*, Stain¹⁹ experimentally obtained for Equation (19) values of $2.3026 A = 5.6$, $B_1 = 5.6$, $B_2 = 0$. These values will be used for numerically evaluating the formulas of the report.

Radial velocity profiles from the Mager model compare well with experimental data for *smooth surfaces* shown in Figures 2 and 3. Results from an eddy-viscosity model by Cooper²³ are also compared in Figure 3.

17. Amfilokhiev, W.B. and A.M. Ferguson, "The Variation of Friction Drag with Surface Roughness in Dilute Polymer Solutions," University of Glasgow, Department of Naval Architecture Experiment Tank Report 8 (Aug 1968).

18. Smallman, J.R. and J.H.T. Wade, "The Influence of Hydrodynamic Drag of High Molecular Weight Compounds," (Canada) C.A.S.I. Transactions, Vol. 2, No. 1, p. 37 (Mar 1969).

19. Stain, W.C., "The Three-Dimensional Turbulent Boundary Layer on a Rotating Disk," Mississippi State University Aerophysics Department, Research Report 35 (Aug 1961).

20. Gadd, G.E., "The Effect on the Turbulent Boundary Layer of Adding Guar Gum to the Water in Which a Disk Rotates," National Physical Laboratory (England), Ship TM 42 (Nov 1963).

21. Cham, T-S. and M.R. Head, "Turbulent Boundary-Layer Flow on a Rotating Disk," Journal of Fluid Mechanics, Vol. 37, Pt. 1, p. 129 (Jun 1969).

22. Erian, F.F., "The Turbulent Flow due to a Rotating Disk," Clarkson College of Technology (Potsdam, N.Y.) Department of Mechanical Engineering (Apr 1970).

23. Cooper, P., "Turbulent Boundary Layer on a Rotating Disk Calculated with an Effective Viscosity," AIAA Journal, Vol. 9, No. 2, p. 255 (Feb 1971).

SKEWNESS OF VELOCITY

As shown in Figure 1, the skewness of boundary-layer flow is given by ψ where

$$\tan \psi = \frac{v_r}{u} \quad (148)$$

At the wall, $z = 0$, $\tan \psi = \alpha$.

The relative skewness is given by $\frac{\tan \psi}{\alpha}$.
For the Prandtl radial-velocity model,

$$\frac{\tan \psi}{\alpha} = g \quad (149)$$

Hence the von Kármán linear model is

$$\frac{\tan \psi}{\alpha} = 1 - \frac{z}{\delta} \quad (150)$$

and the Mager quadratic model is

$$\frac{\tan \psi}{\alpha} = \left(1 - \frac{z}{\delta}\right)^2 \quad (151)$$

Up to the wall, the Goldstein model is

$$\frac{\tan \psi}{\alpha} = \frac{U}{u} - 1 \quad (152)$$

and at the wall, it is

$$\frac{\tan \psi}{\alpha} = 1 \quad (153)$$

The comparison in Figure 4 shows that the Mager model lies between the other two. Since the Mager model is close to the experimental data, it is considered that the flow skewness is overestimated by the von Kármán model and underestimated by the Goldstein model.

LOCAL SKIN FRICTION

The variation of local skin friction parameter σ with Reynolds number is given by Equation (102). Over the usual range of σ (20 to 28), it is determined graphically that $c_3 = 0.9425$, $c_4 = 0.018125$, $c_5 = 0.0854$,

$c_6 = -0.0018$. The local skin friction for the *smooth* case, Equation (102), becomes

$$\sigma = 4.96 \log R - 5.74 \quad (154)$$

This compares very well with the test data shown in Figure 5. The test data for local skin friction were obtained from the velocity profiles by the Clauser procedure.

SKEWNESS OF WALL SHEAR STRESS

The skewness of the wall shear stress α was given by Equation (56); to order $\frac{1}{\sigma}$, it is

$$\alpha = \frac{a_0}{\sigma} \left(1 - \frac{a_1}{\sigma} \right) \quad (155)$$

For *smooth* surfaces with $A_1 = 5.6$, $B_1 = 5.6$, $B_2 = 0$, Equation (57) gives $a_0 = 3.845$ and $a_1 = 1.738$. A close fit obtained graphically over the usual ranges of values of σ produces

$$\alpha = \frac{4.395}{\sigma} - 0.0107 \quad (156)$$

Substitution of Reynolds number R for σ in Equation (102) yields for the *smooth* case

$$\alpha = \frac{4.395}{4.96 \log R - 5.74} - 0.0107 \quad (157)$$

Figure 6 shows a favorable comparison with test data and other predictions. The test data were obtained visually from streak lines that emanated from artificial roughnesses in a sublimation process.²¹

RESISTING MOMENT

The resisting moment coefficient as a function of Reynolds number was given by Equation (71) as

$$\frac{1}{\sqrt{k_m}} = A \log R \sqrt{k_m} + B$$

By a graphical determination, i.e., $c_1 = 0.124$ and i.e. $c_2 = -0.00379$.

For the *smooth* case with $A_1 = 5.6$, $B_1 = 5.6$, and $B_2 = 0$:

$$\frac{1}{\sqrt{k_m}} = 3.456 \log R\sqrt{k_m} - 2.176 \quad (158)$$

Figure 7 indicates a very agreeable correlation with more recent test data which were unavailable at the time of the Goldstein correlation in 1935. There is still need for accurate data at high Reynolds numbers.

RESISTING MOMENT FOR CASE OF MAXIMUM DRAG REDUCTION WITH POLYMER SOLUTION

The development of the interactive layer concept by Virk et al.²⁴ for turbulent shear flows with drag-reducing polymer solutions provides a method of predicting the maximum drag reduction for rotating disks. Such a condition of maximum drag reduction develops if the boundary layer is reduced just to the laminar sublayer next to the wall and the interactive layer. A logarithmic law describes the interactive layer; for rotating disks, it may be written in the circumferential direction as

$$\frac{u}{u_{\tau, \phi}} = \tilde{A} \ln \frac{u_{\tau, \phi} z}{\nu_s} + \tilde{B} \quad (159)$$

where \tilde{A} and \tilde{B} are constants. This equation has the same form as Equation (18) for the smooth case, $B_1 = \text{constant}$.

Hence the torque formula for the smooth case, Equation (71), holds if \tilde{A} is substituted for A and \tilde{B} for B or

$$\frac{1}{\sqrt{k_m}} = \tilde{A} \log R\sqrt{k_m} + \tilde{B} \quad (160)$$

where

24. Virk, P.S. et al., "The Ultimate Asymptote and Mean Flow Structure in Tom's Phenomenon," Transactions American Society of Mechanical Engineers, Journal of Applied Mechanics, Vol. 37, Series E, No. 2 (Jun 1970).

$$\tilde{A} = \frac{\tilde{A}_1 \sqrt{\frac{5}{4\pi}}}{1 - c_2 D} \quad (161)$$

and

$$\tilde{B} = \frac{1}{(1 - c_2 D)} \left[\sqrt{\frac{5}{4\pi}} (\tilde{B} + B_2) - \frac{\tilde{A}}{\sqrt{5\pi}} - \tilde{A}_1 \sqrt{\frac{5}{4\pi}} \log \left(\tilde{F}g \sqrt{\frac{5\pi \tilde{F}^2}{g^2}} \right) + c_1 D \right] \quad (162)$$

$$\tilde{A}_1 = 2.3026 \tilde{A}$$

Since there is no overlapping, $B_2=0$. From Equations (69), (146), and (147), $D = 3.026 \tilde{A}^2/\pi$. From Equations (140), (144), and (143) $\tilde{F}g = 11/18 \tilde{A}$, $\tilde{F}^2 = 2\tilde{A}^2$ and $\tilde{g}^2 = 1/5$. Then

$$\tilde{A} = \frac{\tilde{A}_1 \sqrt{\frac{5}{4\pi}}}{1 - \frac{3.026}{\pi} \tilde{A}^2 c_2} \quad (163)$$

and

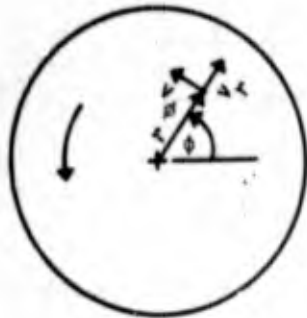
$$\tilde{B} = \frac{1}{\left(1 - \frac{3.026}{\pi} \tilde{A}^2 c_2\right)} \left[\sqrt{\frac{5}{4\pi}} \tilde{B} - \frac{\tilde{A}}{\sqrt{5\pi}} - \tilde{A}_1 \sqrt{\frac{5}{4\pi}} \log \left(\frac{55}{18} \sqrt{2\pi} \tilde{A}^2 \right) + \frac{3.026}{\pi} \tilde{A}^2 c_1 \right] \quad (164)$$

With the values of $\tilde{A}=11.7$ and $\tilde{B} = -17.0$ given by Virk et al.,²⁴ the resisting moment for the case of maximum drag reduction with polymer solutions becomes

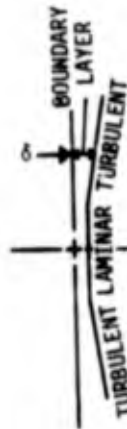
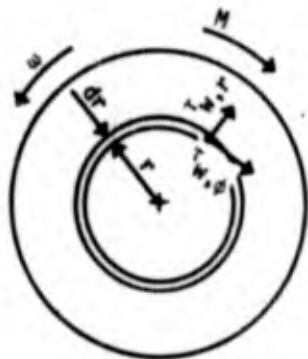
$$\frac{1}{\sqrt{k_m}} = 11.33 \log R_s \sqrt{k_m} - 32.44 \quad (165)$$

Here $R_s \equiv \omega r^2/\nu_s$ where ν_s is the kinematic viscosity of the solution.

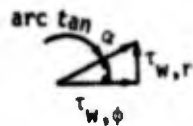
The comparison in Figure 8 shows excellent agreement between Equation (165) and some test data of Hoyt and Fabula.¹⁶



- r = RADIAL DISTANCE
- ϕ = AZIMUTH ANGLE
- z = NORMAL DISTANCE FROM DISK
- v_r = RADIAL VELOCITY
- v_ϕ = CIRCUMFERENTIAL VELOCITY
- v_z = NORMAL VELOCITY

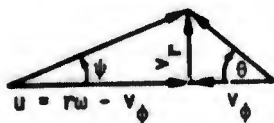


- ω = ANGULAR VELOCITY
- M = RESISTING MOMENT OR TORQUE
- $\tau_{w,r}$ = RADIAL WALL SHEAR STRESS
- $\tau_{w,\phi}$ = CIRCUMFERENTIAL WALL SHEAR STRESS
- δ = BOUNDARY-LAYER THICKNESS



α = SKEWNESS OF WALL SHEAR STRESS, $\alpha = \frac{\tau_{w,r}}{\tau_{w,\phi}}$

SKEWNESS OF FLOW

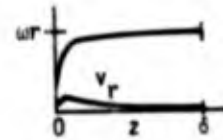


ψ = RELATIVE ANGLE, $\tan \psi = \frac{v_r}{r\omega - v_\phi}$

θ = ABSOLUTE ANGLE, $\tan \theta = \frac{v_r}{v_\phi}$

at $z = 0$, $\tan \theta = 0$, $\tan \psi = \alpha$

TYPICAL VELOCITY PROFILES



$u = \omega r - v_\phi$ = RELATIVE CIRCUMFERENTIAL VELOCITY

Figure 1 - Geometry of Flow and Coordinate System

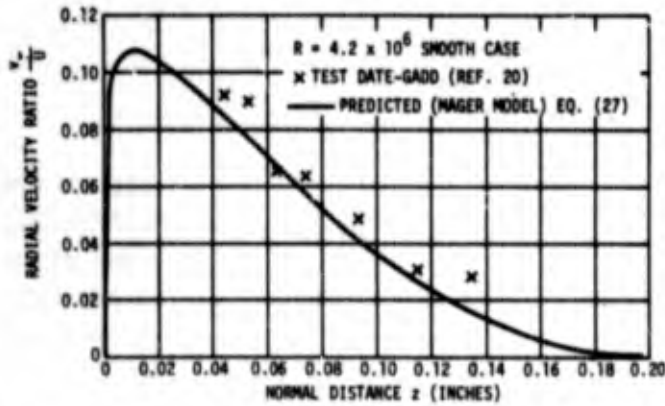


Figure 2 - Radial Velocity Profile Comparison for Smooth Case, $R = 4.2 \times 10^6$

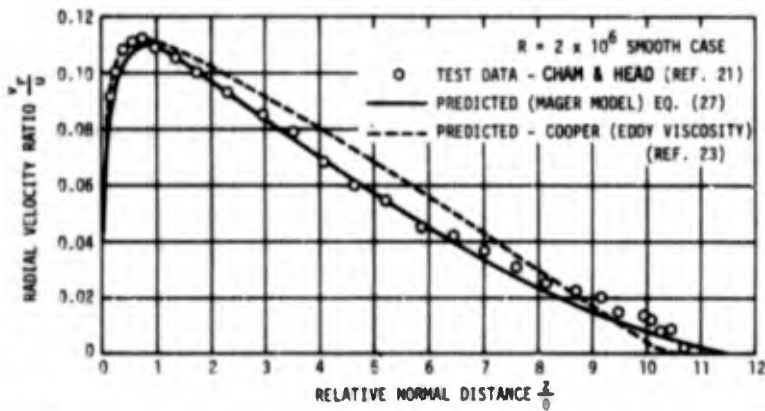


Figure 3 - Radial Velocity Profile Comparison for Smooth Case, $R = 2 \times 10^6$

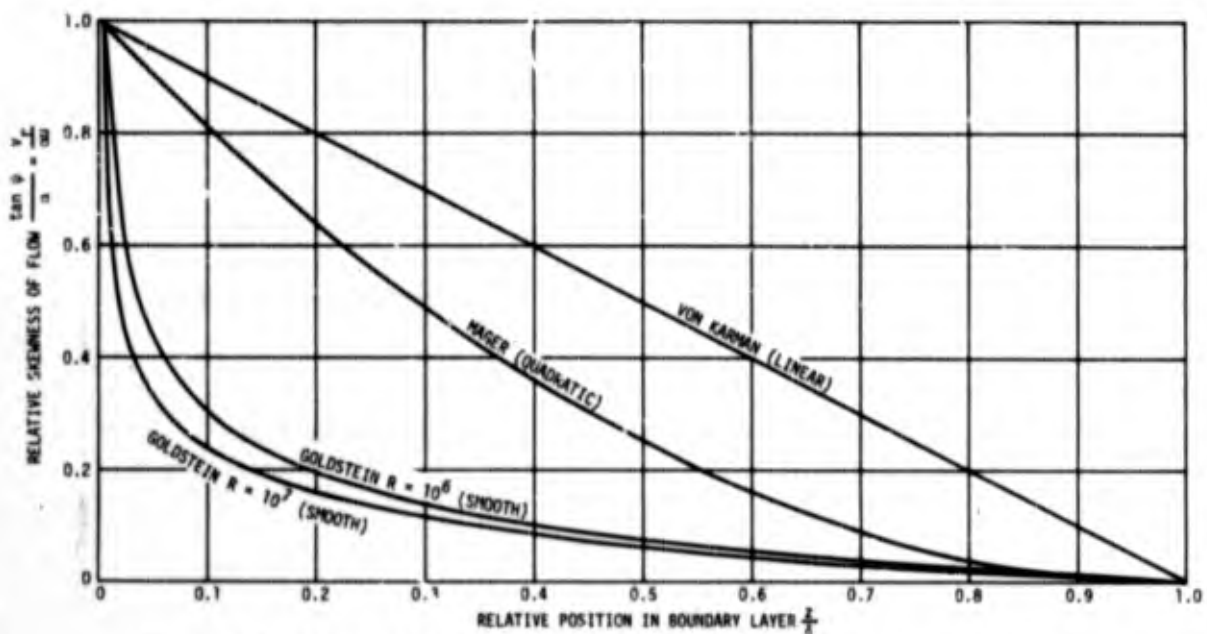


Figure 4 - Comparison of Models of Relative Skewness of Flow

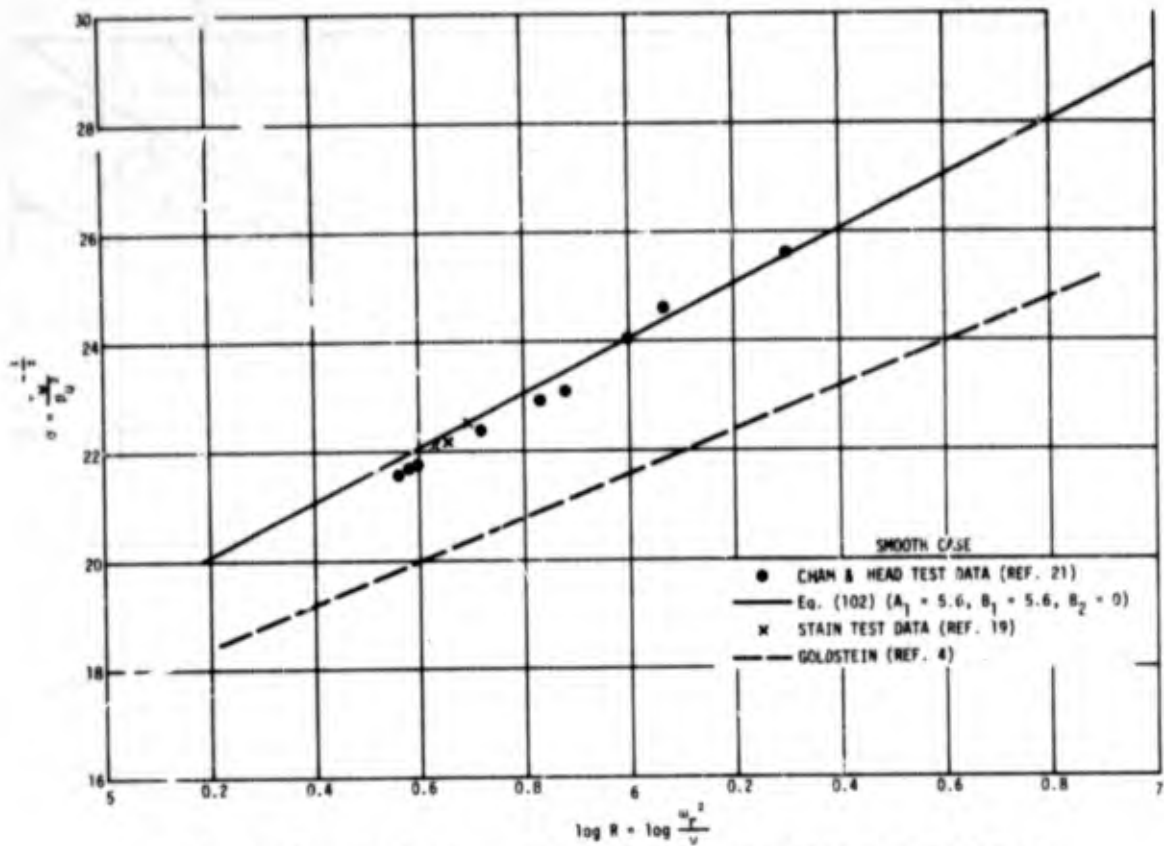


Figure 5 - Variation of Local Skin Friction Parameter σ with Reynolds Number for the Smooth Case

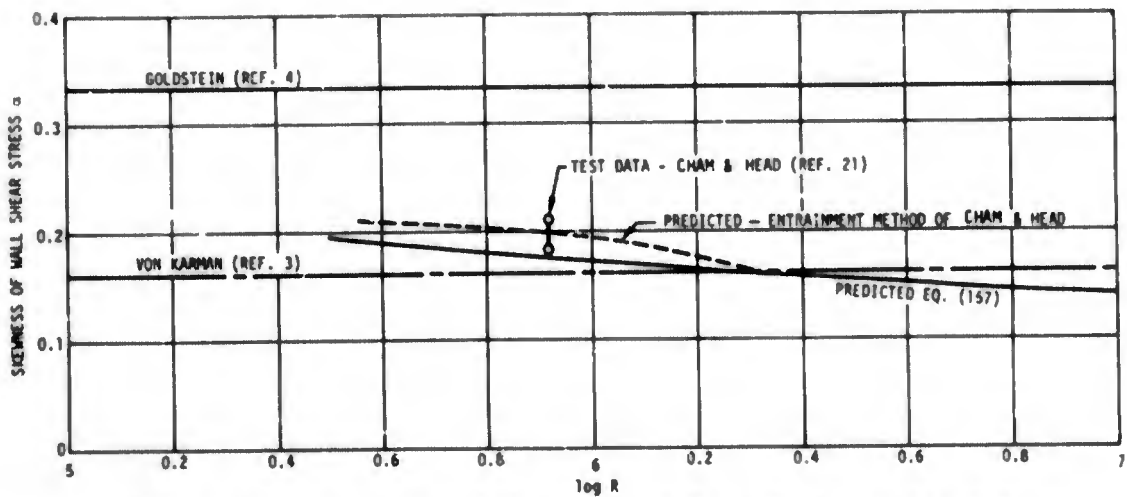


Figure 6 - Variation of Skewness of Wall Shear Stress with Reynolds Number for the Smooth Case

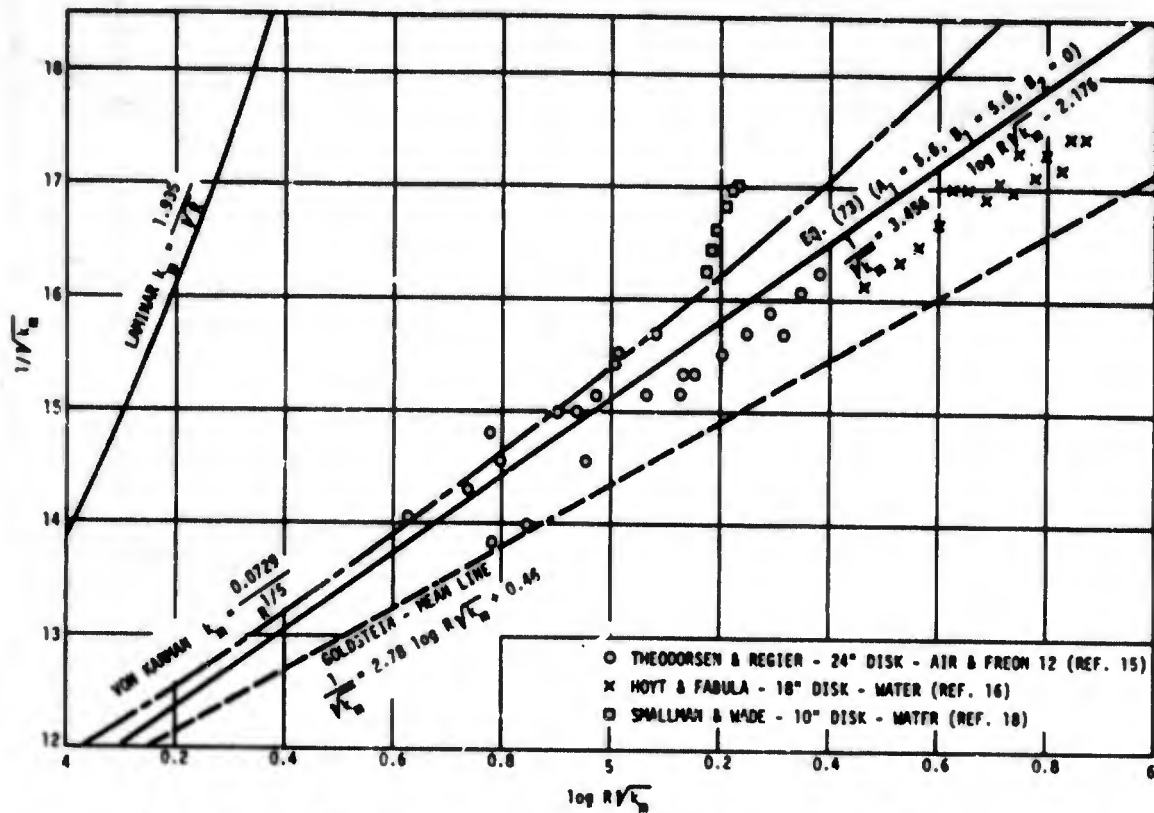


Figure 7 - Moment Coefficient versus Reynolds Number for the Smooth Case

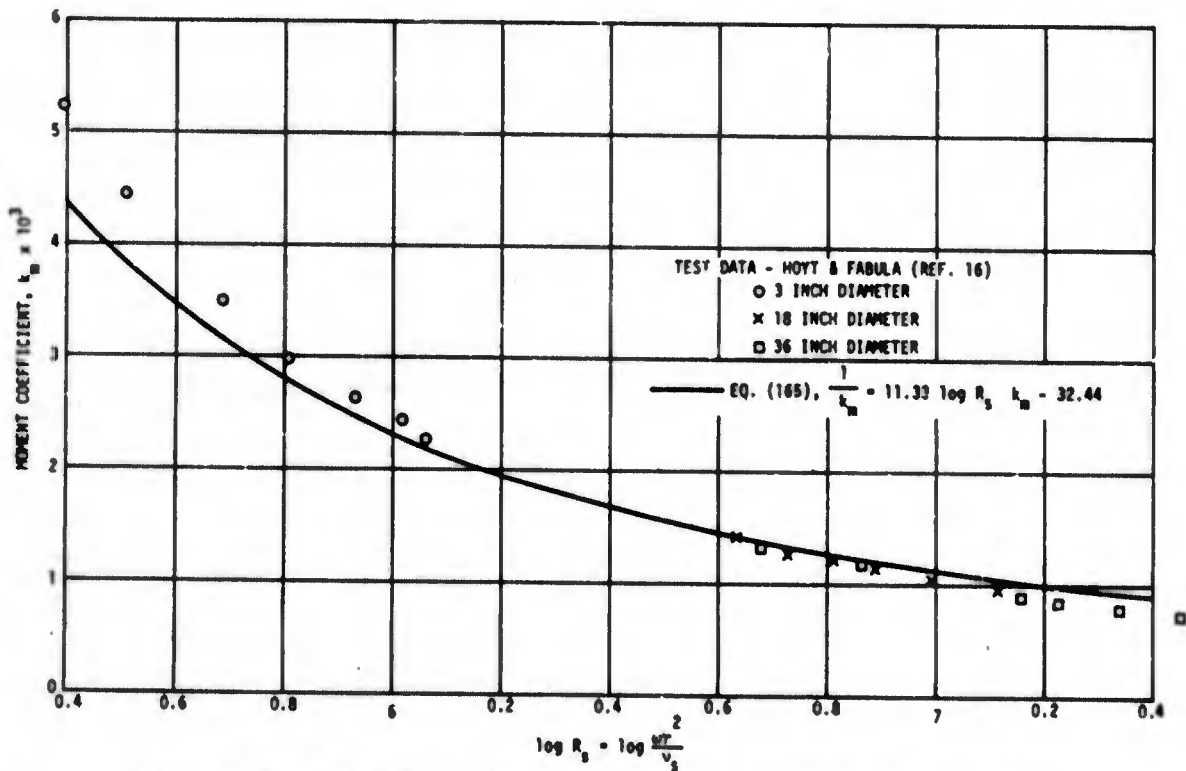


Figure 8 - Maximum Drag Reduction with Polymer Additives

APPENDIX
GENERAL POWER-LAW ANALYSIS FOR *SMOOTH* CASE

It is of interest to repeat the von Kármán analysis for the smooth case with two principal improvements: (1) the power is left arbitrary for the similarity law and (2) the quadratic Mager model is used for the radial velocity profile.

Although von Kármán assumed that the similarity law held for the resultant of the circumferential and radial wall shear stresses, it is preferable to make the simpler assumption that the similarity law holds only for the circumferential wall shear stress. Consequently

$$\frac{u}{u_{\tau, \phi}} = C[n] \left(\frac{u_{\tau, \phi} z}{\nu} \right)^n \quad (A1)$$

where $C[n]$ is a constant for a particular n and n is an arbitrary power.

Then

$$\frac{u}{U} = \left(\frac{z}{\delta} \right)^n \quad (A2)$$

For the radial velocity profile, the Mager model

$$\frac{v_r}{U} = \alpha \frac{u}{U} \left(1 - \frac{z}{\delta} \right)^2$$

becomes

$$\frac{v_r}{U} = \alpha \left(\frac{z}{\delta} \right)^n \left(1 - \frac{z}{\delta} \right)^2 \quad (A3)$$

Substitution of the velocity profiles, Equations (A2) and (A3), into momentum equations, Equations (8) and (9), produces

$$\omega^2 \alpha^2 f_1 \frac{d}{dr} (r^3 \delta) - f_2 r^2 \omega^2 \delta = - r \alpha \frac{\tau_{\omega, \phi}}{\rho} \quad (A4)$$

and

$$\omega^2 \alpha f_3 \frac{d}{dr} (r^4 \delta) = r^2 \frac{\tau_{\omega, \phi}}{\rho} \quad (A5)$$

where

$$f_1 = \frac{1}{2n+1} - \frac{4}{2n+2} + \frac{6}{2n+3} - \frac{4}{2n+4} + \frac{1}{2n+5} \quad (A6)$$

$$f_2 = \frac{2n^2}{(n+1)(2n+1)} \quad (A7)$$

and

$$f_3 = \frac{1}{n+1} - \frac{2}{n+2} + \frac{1}{n+3} - \frac{1}{2n+1} + \frac{2}{2n+2} - \frac{1}{2n+3} \quad (A8)$$

Let

$$\delta = \gamma r^t \quad (A9)$$

where γ and t are constants.

Then

$$\omega^2 \alpha^2 f_1 \gamma(3+t) r^{1+t} - f_2 \omega^2 \gamma r^{1+t} = -\alpha \frac{\tau_{\omega, \phi}}{\rho} \quad (A10)$$

and

$$\omega^2 \alpha f_3 \gamma(4+t) r^{1+t} = \frac{\tau_{\omega, \phi}}{\rho} \quad (A11)$$

From Equations (A10) and (A11),

$$\alpha^2 = \frac{f_2}{(3+t)f_1 + (4+t)f_3} \quad (A12)$$

From the similarity law, Equation (A1), the circumferential wall shearing stress is

$$\frac{\tau_{\omega, \phi}}{\rho} = C^{-\frac{2}{n+1}} (r\omega)^{\frac{2}{n+1}} \nu^{\frac{2n}{n+1}} \delta^{-\frac{2n}{n+1}} \quad (A13)$$

and with Equation (A9),

$$\frac{\tau_{\omega, \phi}}{\rho} = C^{-\frac{2}{n+1}} \omega^{\frac{2}{n+1}} \nu^{\frac{2n}{n+1}} \gamma^{-\frac{2n}{n+1}} r^{\frac{2(1-nt)}{n+1}} \quad (A14)$$

Substitute Equation (A14) into Equation (A11) and equate powers so that

$$t = \frac{1-n}{1+3n} \quad (\text{A15})$$

Then Equation (A12) becomes

$$\alpha^2 = \frac{(1+3n)f_2}{(4+8n)f_1 + (5+11n)f_3} \quad (\text{A16})$$

Also from Equations (A11) and (A14)

$$\gamma = \left[\frac{1+3n}{(5+11n)f_3\alpha} \right]^{\frac{1+n}{1+3n}} C^{-\frac{2}{1+3n}} \left(\frac{v}{\omega} \right)^{\frac{2n}{1+3n}} \quad (\text{A17})$$

Then Equation (A9) becomes

$$\frac{\delta}{r} = \left[\frac{1+3n}{(5+11n)f_3\alpha} \right]^{\frac{1+n}{1+3n}} C^{-\frac{2}{1+3n}} R^{-\frac{2n}{1+3n}} \quad (\text{A18})$$

Also the torque coefficient in Equation (13) becomes

$$k_m = 4\pi f_3\alpha \frac{\delta}{r} = \frac{C_1}{R^{\frac{2n}{1+3n}}} \quad (\text{A19})$$

where

$$C_1 = 4\pi f_3\alpha \left[\frac{1+3n}{(5+11n)f_3\alpha} \right]^{\frac{1+n}{1+3n}} C^{-\frac{2}{1+3n}} \quad (\text{A20})$$

REFERENCES

1. Granville, P.S., "The Frictional Resistance and Turbulent Boundary Layer of Rough Surfaces," *Journal of Ship Research*, Vol. 2, No. 3 (Dec 1958).
2. Granville, P.S., "The Frictional Resistance and Velocity Similarity Laws of Drag-Reducing Polymer Solutions," *Journal of Ship Research*, Vol. 12, No. 3 (Sep 1968).
3. von Kármán, T., "On Laminar and Turbulent Friction," National Advisory Committee for Aeronautics TM 1092 (Sep 1946); translated from *Zeitschrift für angewandte Mathematik und Mechanik*, Vol. 1, No. 4 (Aug 1921).
4. Goldstein, S., "On the Resistance to the Rotation of a Disc Immersed in a Fluid," *Proceedings of Cambridge Philosophical Society*, Vol. 31, Pt. 2, p. 232 (Apr 1935).
5. Dorfman, L.A., "Drag of a Rotating Rough Disk," *Soviet Physics-Technical Physics*, Vol. 3, No. 2, p. 353 (Feb 1958).
6. Dorfman, L.S., "Hydrodynamic Resistance and the Heat Loss of Rotating Solids," *Oliver & Boyd*, London (1963).
7. Prandtl, L., "On Boundary Layers in Three-Dimensional Flow," *B.I.G.S.* 84 (Aug 1946); also *British M.A.P. Report & Translation* 64 (May 1946).
8. Mager, A., "Generalization of Boundary Layer Momentum-Integral Equations to Three-Dimensional Flows Including Those of Rotating Systems," *National Advisory Committee for Aeronautics Technical Report* 1067 (1952).
9. Johnston, J.P., "On the Three-Dimensional Turbulent Boundary Layer Generated by Secondary Flow," *Transactions of American Society of Mechanical Engineers, Journal of Basic Engineering*, Vol. 82, Series D, No. 1 (Mar 1960).
10. Eichelbrenner, E.A., "La Couche Limite Tridimensionnelle en Régime Turbulent d'un Fluide Compressible," *NATO Advisory Group for Aerospace Research AGARDograph* 97 (May 1965).

11. Gregory, N. et al., "On the Stability of Three-Dimensional Boundary Layers with Application to the Flow Due to a Rotating Disk," Philosophical Transactions of Royal Society, London (A) 248, p. 155 (1955); also in "Boundary Layer Effects in Aerodynamics," Symposium at National Physical Laboratory, Great Britain (1955); published by Philosophical Library, New York (1957).
12. Coles, D., "The Law of the Wake in the Turbulent Boundary Layer," Journal of Fluid Mechanics, Vol. 1, Pt. 2 (Jul 1956).
13. Moses, H.L., "The Behavior of Turbulent Boundary Layers in Adverse Pressure Gradients," Massachusetts Institute of Technology Gas Turbine Laboratory Report 73 (Jan 1964).
14. Dryden, J.L. et al., "Hydrodynamics," National Research Council Bulletin 84 (1932); reprinted by Dover Publications, New York, p. 352 (1956).
15. Theodorsen, T. and A. Regier, "Experiments on Drag of Revolving Disks, Cylinders and Streamline Rods at High Speeds," National Advisory Committee for Aeronautics Technical Report 793 (1944).
16. Hoyt, J.W. and A.G. Fabula, "The Effect of Additives on Fluid Friction," 5th Symposium on Naval Hydrodynamics, Office of Naval Research ACR-112, U.S. Government Printing Office, Washington, D.C. (Sep 1964).
17. Amfilokhiev, W.B. and A.M. Ferguson, "The Variation of Friction Drag with Surface Roughness in Dilute Polymer Solutions," University of Glasgow, Department of Naval Architecture Experiment Tank Report 8 (Aug 1968).
18. Smallman, J.R. and J.H.T. Wade, "The Influence of Hydrodynamic Drag of High Molecular Weight Compounds," (Canada) C.A.S.I. Transactions, Vol. 2, No. 1, p. 37 (Mar 1969).
19. Stain, W.C., "The Three-Dimensional Turbulent Boundary Layer on a Rotating Disk," Mississippi State University Aerophysics Department Research Report 35 (Aug 1961).
20. Gadd, G.E., "The Effect on the Turbulent Boundary Layer of Adding Guar Gum to the Water in Which a Disk Rotates," National Physical Laboratory (England), Slip TM 42 (Nov 1963).

21. Cham, T-S. and M.R. Head, "Turbulent Boundary-Layer Flow on a Rotating Disk," *Journal of Fluid Mechanics*, Vol. 37, Pt. 1, p. 129 (Jun 1969).

22. Erian, F.F., "The Turbulent Flow due to a Rotating Disk," Clarkson College of Technology (Potsdam, N.Y.) Department of Mechanical Engineering (Apr 1970).

23. Cooper, P., "Turbulent Boundary Layer on a Rotating Disk Calculated with an Effective Viscosity," *AIAA Journal*, Vol. 9, No. 2, p. 255 (Feb 1971).

24. Virk, P.S. et al., "The Ultimate Asymptote and Mean Flow Structures in Tom's Phenomenon," *Transactions American Society of Mechanical Engineers, Journal of Applied Mechanics*, Vol. 37, Series E, No. 2 (Jun 1970).